Micromachined III-V Multimorph Actuator Model and Design Using Simulated Annealing (SA)-Based Global Optimization

A. Ongkodjojo[a], F. E. H. Tay[a,b] and R. Akkipeddi[c]

[a]Micro- & Nano-Systems Cluster, Institute of Materials Research & Engineering (IMRE)
3 Research Link, Singapore, an-ong@imre.a-star.edu.sg
[b]Department of Mechanical Engineering, NUS, Singapore, mpetayeh@nus.edu.sg
[c]Opto- & Electronic Systems Cluster, IMRE, Singapore, ram-akki@imre.a-star.edu.sg

ABSTRACT

A new AlAs/GaAs-based multimorph microactuator is designed and modeled for micro-opto-electro-mechanical systems (MOEMS) applications with photonic devices. As the piezoelectric-based III-V materials such as AlAs/GaAs have small piezoelectric constants, we have developed the Simulated Annealing (SA)-based global optmization to obtain the optimum solution for the structure with a high sensitivity. This proposed optimization method can efficiently lead the design for achieving the highest sensitivity as the structure materials can be grown epitaxially with a minimum thickness of 10 nm for each layer. Therefore, the smallest thickness of the structure layers and its highest sensitivity can easily be achieved by using the optimization method. In addition, for more realistic design and model, we develop the constraint optimization method using the SA algorithm, which can satisfy the specified constraints.

Keywords: global optimization, Simulated Annealing (SA), III-V multimorph, MOEMS, AlAs/GaAs

1 INTRODUCTION

The micro-opto-electro-mechanical systems (MOEMS) are currently in a good progress in many fields [1] and using silicon material for their functionalities because of good mechanical properties, less processing difficulties, and low cost of the material. However, with no optoelectrical properties for the material, it is highly promising to consider III-V materials integrated with MEMS devices, which have already made a tremendous impact in optoelectronics and high frequency devices, and communication fields and industries. Detailed investigations of the materials have been dealt by various authors in the literature [2]. As we use the piezoelectric means for actuation, piezoelectric-based III-V materials such as AlAs/GaAs are used for our mechanical structures.

In this research work, a multimorph microactuator is proposed and developed, which provides high sensitivity, big generative force, good strength, and high natural frequency for MEMS applications with relatively small piezoelectric coefficients, especially for MOEMS applications. Besides, the multimorph models provide better validation to the experimental data as they consider more detailed models including all of the thin films [3]. According to our best knowledge, there is no literature on multimorph or bimorph using the same material such as AlAs/GaAs for MEMS applications.

As the piezoelectric-based III-V materials have small piezoelectric constants, the SA-based global optmization has been proposed to obtain the optimum solution without violating the specified constraints [4]. For more realistic designs, some constraints are imposed to satisfy mechanical and electrical requirements as well as micro-fabrication process capabilities and limitations.

2 MATHEMATICAL MODELING

In this section, we present a mathematical model of a novel piezoelectric multimorph structure, which is made of two piezoelectric layers, a middle layer, and some electrode layers with parallel electrical connections. Our proposed structure is shown in Fig. 1. The middle layer, which plays an elastic role in addition to its electrical function, has been inserted between the two piezoelectric layers for improving the strength of our structure.

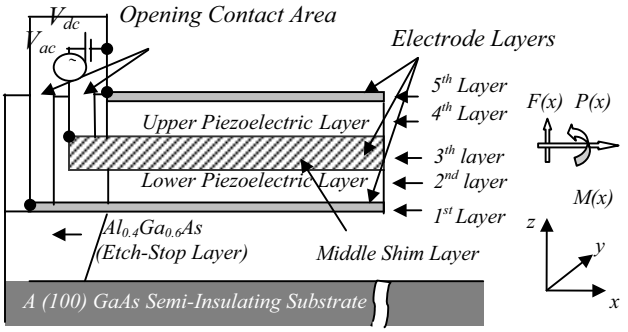

Figure 1: AlAs/GaAs-based multimorph microactuator

As large displacements are needed for our optical MEMS applications, the magnitude of deflection of the actuator will be investigated in the form of a sensitivity parameter. Therefore, we focus on the sensitivity as our single objective function in order to obtain high sensitivity for our actuator applications.

When a driving voltage is applied to a piezoelectric material, the material structure will be deflected. The

electric field is non-zero only for piezoelectric layers. The structure will tend to contract in the *x*-*y* plane, and expand along the electric field, which is applied in parallel with the polarization of the material along the *z*-axis. For example, the upper piezoelectric material expands while the lower piezoelectric material contracts as a result of the electric field, resulting in a bending in the downward direction. However, the structure will deform in the opposite direction as an alternate driving voltage is applied to the multimorph. Thus, the microactuator will vibrate dynamically, when the AC driving voltage V_{ac} is applied with a driving frequency.

Generally, the piezoelectric effect of the structure is expressed by [5]:

$$S_{ij} = s^{E}_{ijkl} T_{kl} + d_{kij} E_k \tag{1}$$

$$D_i = d_{ikl} T_{kl} + \varepsilon^{T}_{ik} E_k \tag{2}$$

where S_{ij}, s^{E}_{ijkl}, T_{kl}, d_{kij}/d_{ikl}, E_k, D_i, and ε^{T}_{ik} are strain, elastic compliance constant at constant electric field, stress, the piezoelectric constant, electric field, electric displacement, and permittivity at constant stress, respectively.

By imposing force and moment equilibrium on the structure, the deflection of the proposed multimorph can be obtained as given by [6]:

$$z(x) = \frac{x^2}{2} \frac{\left(-\sum_{n=1}^{N} d_{31-n} E_n A_n Z_{n-g} E_{e-n} \right)}{\left(\sum_{n=1}^{N} E_n \left[I_n + A_n Z^2_{n-g} \right] \right)} \tag{3}$$

where x is the length of the multimorph; d_{31-n} is the transverse piezoelectric coefficient for the n^{th} piezoelectric layer ($d_{31-n} = d_{31-n}(1 + \nu_n)$); E_n is the effective Young's modulus for the n^{th} layer ($E_n = E_n/(1 - \nu_n^2)$), where ν_n is Poisson's ratio for the n^{th} layer; A_n is the area of n^{th} layer cross section; $Z_{n-g} = (z_n - z_g)$ is the new coordinate, which considers the neutral or global axis; E_{e-n} is the electric field; and I_n is the moment inertia for the n^{th} layer. For obtaining the deflection equation, we use a relationship between the curvature $1/R$ and the displacement $z(x)$ by $1/R(x)=d^2z(x)/dx^2$ for small displacements, where R is the radius of the curvature.

Then, the natural frequency of the structure ω_n is derived using the equivalent stiffness k_{eq} and the mass of the multimorph m_b as expressed by:

$$\omega_n = (\beta l)^2_n \left(\frac{k_{eq}}{m_b} \right)^{\frac{1}{2}} \tag{4}$$

where $(\beta l)_1^2$ is a constant of 3.5160 for the first mode of the natural frequency [7]. Finally, the quality factor due to the squeeze film damping of the structure considering gas rarefaction effects has been investigated [4, 8].

3 GLOBAL OPTIMIZATION

The optimal design of our proposed multimorph is carried out to find the maximum sensitivity while satisfying some constraints imposed by functional and geometrical constraints. A method of global optimal design with Simulated Annealing (SA) is used in this research work. The SA is an efficient and adaptive search method applicable to real-life constrained optimization problems. It is analogous to the physical annealing process where an alloy is cooled gradually so that a minimal energy state is achieved. The method avoids getting stuck in local optima and keeps track of the best overall objective function value overall, thereby, resulting in efficient global search strategies. In the design process, the optimization problem is formulated to find the design variables so that the objective function is maximized, while satisfying the multidisciplinary design constraints, including both mechanical and electrical requirements as well as microfabrication limitations/capabilities. More details on the optimization method have been reported [4].

3.1 Design Variables

To select the design variables, the influence of each parameter to the sensitivity should be analyzed. The design variables are the length, the width, and the height of each layer of the multimorph actuator as presented in Table 1. The influence of each design parameter can be decided through Eq. (3).

Variable	Description	Reasonable Range	
		Minimum	Maximum
l_b (μm)	Length	5×10^1	1×10^2
w_b (μm)	Width	5	1×10^1
h_{p1} (μm)	Height (AlAs)	1×10^{-2}	5
h_{p2} (μm)	Height (GaAs)	1×10^{-2}	5
h_m (μm)	Height (inner electrode)	1×10^{-2}	5
h_e (μm)	Height (outer electrode)	1×10^{-2}	3
V_{dc} (V)	DC bias voltage	0	5
V_{ac} (V)	AC voltage	0	1

Table 1: Design variables for the multimorph

3.2 Constraints

In the design process of the constrained nonlinear optimization, constraints need to be identified and defined correctly. Generally, constraint expressions involve both dependent and independent design variables as well as explicit bounds on the variables. Some constraints, which are used in this research work, have been derived from [4]

such as the natural frequency, the quality factor, the output linearity, and the support beam buckling. Under certain fabrication conditions, the microstructure can collapse and permanently adhere to their underlying substrates. In order to avoid stiction, collapse, and contact with the substrate, real and practical design constraints of our proposed multimorph microactuator must be taken into account. Therefore, we present the additional constraints such as other geometrical constraints, stiction, contact during fabrication, and collapse in this paper.

Stiction may occur whenever flexible and smooth structures are brought in contact with the substrate. It is clear that stiction can easily cause malfunctioning in our actuator. In order for the actuator to snap back after contacting the substrate, the length of the beam must be shorter than the critical length ($l_{cr\text{-}s}$), which is expressed by [9]:

$$l_{cr-s} = \sqrt[4]{\frac{3}{8}\frac{E\left(h_{p1}+h_{p2}+h_m+2h_e\right)^3 g^2}{\gamma_s}} \quad (5)$$

where γ_s is adhesion energy per unit area or surface tension, which is assumed to be approximately 0.11 J/m^2 [10].

During the drying process after wet sacrificial layer etching, the structure is being pulled against the substrate surface by strong capillary forces. It is more practical to avoid contact during the drying process. To avoid contact, which is bridging a part of the beam area flat against the substrate surface, the critical length given by Eq. (6) must be considered.

$$l_{cr-c} = \sqrt[4]{\frac{3}{16}\frac{E\left(h_{p1}+h_{p2}+h_m+2h_e\right)^3 g^2}{\gamma_{la}\cos\theta_c}} \quad (6)$$

where $\gamma_{la} \cos \theta_c$ is the adhesion energy of the liquid bridge per unit area, which is assumed to be approximately 0.11 J/m^2. However, this constraint can be neglected, when a dry sacrificial etching process is chosen for the fabrication process.

As our actuator can be applied to a class of wavelength tunable electro-optic devices, a micro-mirror can be attached to the actuator for the real applications. Therefore, we need to consider our actuator to be loaded at its tip by an applied external force (***n*** times its own weight). In this case, we can model that our actuator is loaded by a force of ($n\rho w_b(h_{p1}+ h_{p2}+h_m+2h_e)l_b a$), when the substrate is accelerated by a in an upward direction. Thus, the critical length of the actuator is expressed by [9]:

$$l_{cr-load} = \sqrt[4]{\frac{Eg\left(h_{p1}+h_{p2}+h_m+2h_e\right)^2}{4n\rho a}} \quad (7)$$

4 RESULTS AND DISCUSSION

The computational results of the global optimization for the structure are shown in Fig. 2 and Table 2. These computational results are presented with a driving frequency of 530 kHz, an air pressure, and an applied force of 50 μN. Fig. 2 shows the results of the SA run, where the solution has converged to the global maximum. As the temperature falls, one can observe that the algorithm closes in on the global maximum. According to Table 2, the design variables give a maximum value of 3.4 nm/V for the sensitivity of the multimorph, while satisfying the imposed constraints.

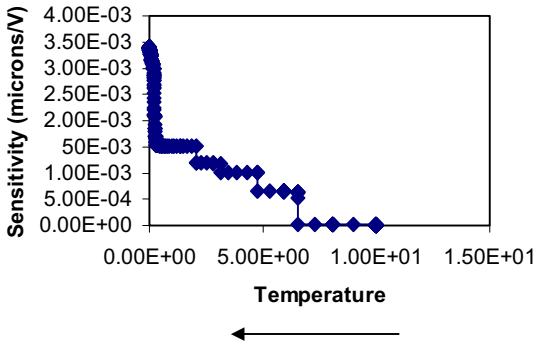

Figure 2: Sensitivity value converged using the SA

Variable	Description	Results
l_b (μm)	Length	7.175 x 10^1
w_b (μm)	Width	1.0 x 10^1
h_{p1} (μm)	Height (AlAs)	7.89 x 10^{-1}
h_{p2} (μm)	Height (GaAs)	4.98 x 10^{-1}
h_m (μm)	Height (inner electrode)	2.71
h_e (μm)	Height (outer electrode)	1.0 x 10^{-2}
V_{dc} (Volt)	DC bias voltage	4.3
V_{ac} (Volt)	AC voltage	7.136 x 10^2
	Geometrical Constraints	
z (μm)	Deflection	1.705 x 10^{-2}
h_{p1}+h_{p2}+h_m+2h_e	Total height	4.013
R (μm)	Curvature (radius)	1.5096 x 10^5
	Functional Constraints	
ω_z (rad/s)	Resonant frequency	3.3313 x 10^6
Q_z	Quality factor	2.525 x 10^2
0.8*$l_{cr\text{-}b}$ (μm)	Support beam buckling	1.324 x 10^2
0.8*$l_{cr\text{-}s}$ (μm)	Stiction	9.32 x 10^1
0.8*$l_{cr\text{-}c}$ (μm)	Contact (fabrication)	7.84 x 10^1
0.8*$l_{cr\text{-}l}$ (μm)	Collapse (loading)	7.175 x 10^1
	Objective Function	
S (μm/V)	Maximum sensitivity	3.395 x 10^{-3}

Table 2: Global optimization results for the multimorph

To ensure that our models and designs are valid and accurate, the optimization results were verified with the FEA using ANSYS^{TM}. A coupled-field multiphysics

analysis that accounts for the interaction between electric and structural fields was run. The 3-D model uses SOLID5 elements (brick 8-node element, 3-D coupled field element) for the piezoelectric layers and SOLID45 element (3-D structural element) for the middle shim layer as used by the modal analysis. Then, an input positive voltage is applied in parallel to the piezoelectric layers. Material property data for the dielectric constant matrix ($[\varepsilon/\varepsilon_0]$, where ε_0 = 8.85 x 10^{-12} F/m), the piezoelectric stress coefficient matrix [*e*], and the anisotropic elastic coefficient matrix [*c*] have been reported [2]. For obtaining the elastic coefficient matrix [e], $c_{11} = c_{22} = c_{33} = 1/s_{11}^E = E$, N/m^2/Pa are inputs. While, the piezoelectric stress coefficient matrix [*e*] has been calculated by using the relationship between the piezoelectric strain coefficient matrix [*d*] and a compliance coefficient S_{44}, where S_{44} = 1.7 x 10^{-11} m^2/N and 1.68 x 10^{-11} m^2/N for Alas and GaAs respectively.

According to Table 3 and Fig. 3, there is an agreement among the mathematical modeling, the proposed models, and the finite element modeling. The discrepancies (as shown in Fig. 3) are caused by the fact that the derived mathematical modelings did not consider the piezoelectric effect of the structure width. Considering the piezoelectric effect across the model width, there is an excellent agreement between the SA and the FEA results. In addition, the validity of our designs have been confirmed by Fig. 5 (resonance frequency as a function of the cantilever microbeam length for GaAs) of the paper [11]. Therefore, very high resonance frequencies can be achieved by the small dimension (length) of the structure by using the growth control in III-V materials.

Mode	SA Result (Hz)	FEA Result (Hz)	Error (%)
1st	5.3162 x 10^5	5.4581 x 10^5	2.60
2nd	-	1.3472 x 10^6	-
3rd	-	3.3919 x 10^6	-

Table 3: Verification summary of the natural frequency

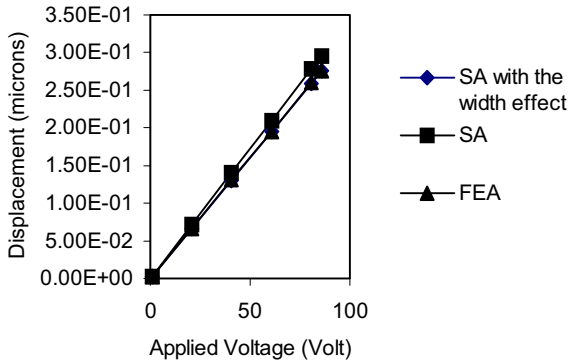

Figure 3: Comparison between our multimorph model and FEA simulation results using ANSYS™

5 CONCLUSION

Based on the global optimization, the best design has been globally the optimum design, while satisfying the multidisciplinary design constraints imposed by mechanical and electrical requirements as well as III-V microfabrication process capabilities and limitations. These constraints have made our proposed design to be visible and real for our applications.

Based on the design, the AlAs/GaAs-based microactuator has a sensitivity of 3.4 x 10^{-3} μm/V with a resonance frequency of 530 kHz and a quality factor of 253 in air without violating the multidisciplinary design constraints. In addition, the valid driving voltage range of the applied DC voltage (V_{dc}) is 0 – 87.5 Volt with a fixed applied AC voltage (V_{ac}) of 714 mV for deflecting the structure up to 10% of the gap. Considering the breakdown field of the piezoelectric materials, the valid driving DC bias voltage is up to about 20 Volts, which can be applied to the material structure.

The III-V materials-based multimorph shows potential applications for monolithic integration of optoelectronic components with MEMS devices enabling the realizations of MOEMS.

ACKNOWLEDGEMENTS

The authors are grateful to A*STAR (Agency for Science, Technology, and Research), Singapore for their funding. This work is supported by the A*STAR under the SERC Grant No.0221070006: III-V Optical MEMS Project.

REFERENCES

[1] H. Fujita and H. Toshiyoshi, IEICE Trans. Electron., E83-C, 9, 1427 – 1434, 2000.
[2] S. Adachi, J. Applied Physics, 58-3,1 – 29, 1985.
[3] D. L. DeVoe and A. P. Pisano, J. Microelectromech. Sys., 6-3, 266 – 270, 1997.
[4] A. Ongkodjojo and Francis E. H. Tay, J. Micromech. Microeng., 12, 878 – 897, 2002.
[5] IEEE Standard on Piezoelectricity – An American National Standard, ANSI/IEEE Std, 176-1987.
[6] E. B. Tadmor and G. Kosa, J. Microelectromech. Sys., in press, 2003.
[7] Thomson W and Dahleh M, "Theory of Vibrations with Applications," Englewood Cliifs, NJ: Prentice Hall, 1998.
[8] A. Ongkodjojo and Francis E. H. Tay, Int. J. Comp. Eng. Sci. (IJCES) – Symposium G:MEMS – ICMAT 2003, Singapore, in press.
[9] N. Tas, T. Sonnenberg, H. Jansen, R. Legtenberg, and M. Elwenspoek, J. Micromech. Microeng. 6, 385 – 397, 1996.
[10] F. Shi, S. MacLaren, C. Xu, K. Y. Cheng, and K. C. Hsieh, J. Applied Physics, 93-9, 5750 – 5756, 2003.
[11] H. Ukita, Y. Uenishi, and H. Tanaka, Science, 260-5109, 786 – 789, 1993.